Faraday Discussions
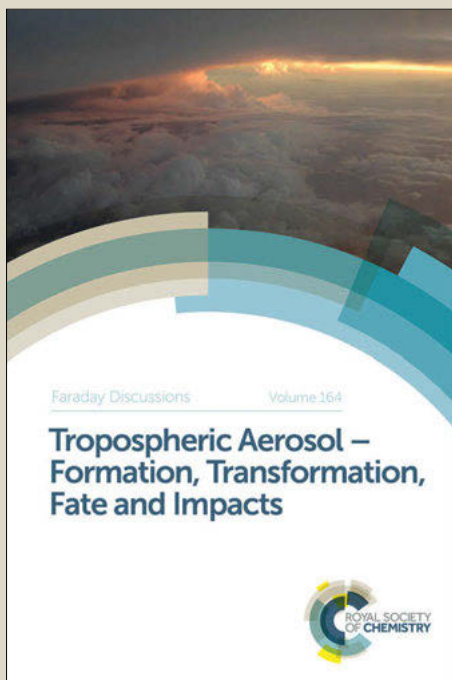
This manuscript will be presented and discussed at a forthcoming Faraday Discussion meeting.
All delegates can contribute to the discussion which will be included in the final volume.

Register now to attend! Full details of all upcoming meetings: http://rsc.li/fd-upcoming-meetings

Faraday Discussions   Volume 164

Tropospheric Aerosol – Formation, Transformation, Fate and Impacts

ROYAL SOCIETY OF CHEMISTRY

ROYAL SOCIETY OF CHEMISTRY

www.rsc.org/faraday_d

Journal Name

ARTICLE

Electro-deposition and re-oxidation of carbon in carbonate containing molten salts

Happiness V. Ijije, Richard C. Lawrence, Nancy J. Siambun, Sangmun Jeong, Daniel A. Jewell, Di Hu and George Z. Chen*

Electrochemical deposition and re-oxidation of solid carbon were studied in CO_3^{2-} ion containing molten salts (e.g. $CaCl_2$-$CaCO_3$-$LiCl$-KCl and Li_2CO_3-K_2CO_3) at temperatures between 500 and 800 °C under Ar, CO_2 or N_2-CO_2 atmospheres. Electrode reactions were investigated by thermodynamic analysis, cyclic voltammetry and chronopotentiometry in a three-electrode cell under various conditions. The findings suggest that electro-reduction of CO_3^{2-} is dominated by carbon deposition on all three tested working electrodes (Ni, Pt and mild steel), but partial reduction to CO can also occur. Electro-re-oxidation of the deposited carbon in the same molten salts was investigated for potential applications in, for example, direct carbon fuel cells. A brief energy and cost analysis is given based on results from constant voltage electrolysis in a two-electrode cell.

Introduction

Electrochemical reduction of the carbonate ion (CO_3^{2-}) to solid carbon in molten salts has been known possibly since mid-1960s.[1,2] It then gained only a limited interest,[3,4] possibly because of the readily availability of various forms of carbon from fossil resources and biomass. However, in recent years renewed interests have grown fairly fast [5-11] due to largely the needs to reduce CO_2 emission to avoid the detrimental climate change and, more importantly, to utilise this waste gas as a carbon source for synthesis and processing of materials and chemicals, such as steel carburisation and production of the so called solar fuels.[8,12] In fact, solar fuel production can be regarded as an energy storage process that is very suitable for remote and seasonal purposes. Yet, considering its high energy content, carbon production from CO_2 is far better for energy storage (ΔH^o = -25.97 MJ/L at 20 °C for a carbon powder packed to 0.792 g/mL in apparent density) in comparison with, for example, methanol production from CO_2 and H_2O (ΔH^o = -16.71 MJ/L at 20 °C for liquid CH_3OH of 0.792 g/mL in density).[13] This simple thermodynamic comparison formed the basis of our research programme since 2006.[14] Herein we summarise our findings on electro-deposition of solid carbon from molten salts under CO_2 containing atmospheres,[8,11] and report for the first time our investigation on electrochemical oxidation of the electro-deposited carbon in molten salts.

The molten salt suitable for electrolytic production of carbon from CO_2 should be able to dissolve the O^{2-} ion which is a product from carbon deposition, and also helps to absorb CO_2

and convert it to the CO_3^{2-} ion. Because of their low costs and environmental impacts, both chloride and carbonate salts, particularly their mixtures were investigated in this laboratory.[8,11] It has been observed that electro-deposition of carbon can proceed in all tested molten salt combinations, as long as Li^+ ions are present.[1-4] In other cases, deposition is not impossible, but occurs at much lower rates.[15] This phenomenon may be accounted for by the relative deposition potential of Li, Na, or K metal compared with that of carbon as expressed by the following reactions.

$$2M_2CO_3 = 4M + 2CO_2 + O_2 \quad (M = Li, Na \text{ or } K) \quad (1)$$
$$3M_2CO_3 = C + 3M_2O + 2CO_2 + O_2 \quad (2)$$
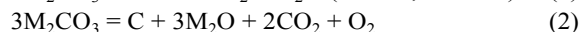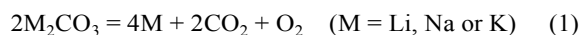
Note that reaction (2) is actually the sum of the following reactions (3) and (4)×2 .

$$M_2CO_3 = C + M_2O + O_2 \quad (3)$$
$$M_2CO_3 = M_2O + CO_2 \quad (4)$$

This combination is to aid electrochemical analysis since both reactions (1) and (2) have the same anodic reaction (5) below.

$$2CO_3^{2-} = 2CO_2 + O_2 + 4e \quad (E^o = 0 \text{ V}) \quad (5)$$

The potentials of reactions (1) and (2) against reaction (5), i.e. a hypothetic reference electrode of CO_3^{2-}/CO_2-O_2, are listed in Table 1 [13] which shows that in molten alkali carbonates, carbon deposition is thermodynamically preferred to Li deposition, but

Table 1. Deposition potentials (vs. CO_3^{2-}/CO_2-O_2) of alkali and alkaline earth metals via reactions (1), and carbon via reaction (2) in their own molten carbonate salts at 600 °C.

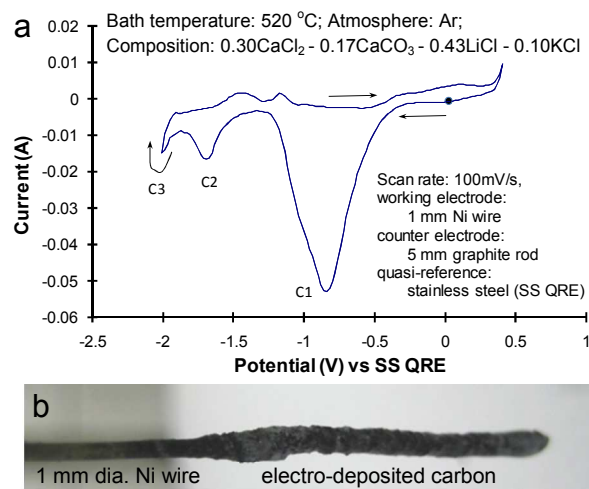| Molten salt	Alkali metal	Carbon
Li_2CO_3	-2.964 V	-1.719 V
Na_2CO_3	-2.546 V	-2.551 V
K_2CO_3	-2.612 V	-3.083 V
$CaCO_3$	-3.033 V	-1.349 V
$BaCO_3$	-3.069 V	-1.992 V

Fig. 1. (a) Cyclic voltammogram (CV) of a nickel wire in a quaternary molten salt bath. Experimental conditions are indicated with the bath composition in molar ratio. The potential scan started cathodically from 0 V as indicated by the round solid spot on the CV. (b) A photograph showing the Ni wire working electrode (1 mm dia.) with deposited carbon after recording two consecutive CVs.

more difficult than Na or K deposition, which is in line with experimental observations of the authors and others.[1-4,15] (With reference to CO_3^{2-}/CO_2-O_2, in the following discussion, the standard potential, E^o, provided next to the electrode reaction is for the reaction occurring in pure molten Li_2CO_3 at 600 °C.)

Previous studies of electro-deposition of carbon were mostly carried out in molten alkali metal salts. However, thermodynamic calculations show that it is also possible to use molten alkaline earth metal salts. It can be seen in Table 1 that carbon deposition is also preferred to alkaline earth metal deposition in both molten $CaCO_3$ and $BaCO_3$. However, $CaCO_3$ decomposes at temperatures only slightly above its melting point (825 °C). $MgCO_3$ is even worse and decomposes at temperature below 350 °C before melting, which is the reason why Table 1 does not contain data for $MgCO_3$. $BaCO_3$ is thermally more stable but it is expensive to use, whilst barium salt toxicity is also a concern. Nevertheless, in this work, it was found that electro-deposition of carbon could be achieved in the molten mixture of $CaCl_2$ and $CaCO_3$ (84:16 in molar ratio) at temperatures higher than 730 °C. To lower the working temperature, mixtures of chlorides were used in some cases to dissolve $CaCO_3$ and enable electro-deposition of carbon.

Experimental

Details of chemicals, materials, experimental equipment, set up and procedures can be either found in previous publications from this laboratory,[8,11,17] or are specified in this paper.

Results and discussion

Fig. 1a presents the cyclic voltammogram (CV) of a Ni wire working electrode in the quaternary mixture of 0.30 $CaCl_2$ - 0.17 $CaCO_3$ - 0.43 LiCl - 0.10 KCl in molar ratio. The CV was recorded under argon, instead of CO_2, so that if carbon deposition may occur, it can be attributed without doubt to the reduction of the CO_3^{2-} ion. The most prominent feature of the CV in Fig. 1a is an almost symmetrical and large reduction current peak C1. To confirm carbon deposition, the Ni wire working electrode was removed from the molten salt bath after recording two consecutive CVs similar to that in Fig. 1a. A carbon coating was clearly seen on the Ni wire as evidenced by the photograph in Fig. 1b. According to Table 1, peak C1 can

be attributed to carbon deposition because its potential was less negative than those of the other two reduction peaks (C2 and C3). The relative potentials of C2 and C3 to that of C1 suggest K and Li deposition, respectively. Deposition of Ca requires a more negative potential and hence did not appear on the CV.

To enhance carbon deposition, electrolysis was carried out in a two electrode cell under different CO_2 partial pressures. The cathode was a mild steel rod of 5.0 mm dia., and the anode was a SnO_2 rod of 10.0 mm dia. which functioned as an inert anode.[16] A high cell voltage (4.0 V) was applied to gain a high deposition rate. The molten salt bath temperature was also increased to 579 °C for the same reason. The electrolysis current was observed to increase with the CO_2 partial pressure as exemplified in Fig. 2a, in agreement with the reduction (6) and regeneration (7) of CO_3^{2-} ions as follows:

$$CO_3^{2-} + 4e = C + 3O^{2-} \quad (C1, E^o = -1.719 \text{ V}) \quad (6)$$
$$CO_2 + O^{2-} = CO_3^{2-} \quad (7)$$
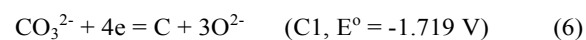
Note that the bath compositions differ slightly in Fig. 1a and Fig. 2a, which was not intentional, but due to the inconvenience to prepare the multicomponent molten salt bath. To compare the results, electrolysis was terminated at 1 h, and the cathode was removed from the bath. Fig. 2b displays a photograph of the cathodes, showing an increasing thickness of the deposited carbon coating with increasing the CO_2 partial pressure.

It is interesting to note in Fig. 2b that the surface of the deposited carbon was covered by small craters that were strong evidence of gas bubbles being formed on the cathode during electrolysis. This was thought to be CO formation via reaction (8). If not escaping from the molten salt, CO may undergo further changes on the electrode via reactions (9) and/or (10).
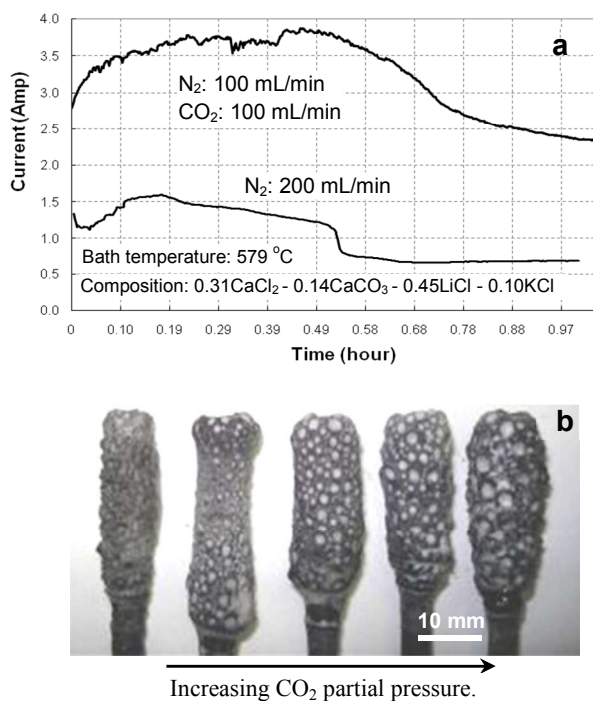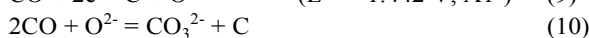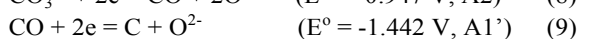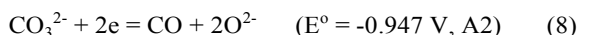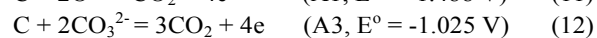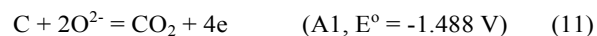
Fig. 2. (a) Current-time plots recorded during constant voltage (4.0 V) electrolysis in a quaternary molten salt bath with a mild steel cathode (5 mm dia. rod) and a SnO_2 anode (10 mm dia. rod) under different atmosphere as indicated. (b) The mild steel rod cathodes with carbon deposits collected after 1 h electrolysis. The electro-deposition on each cathode was carried out consecutively in the same bath, but under different ratios of N_2 and CO_2 flow rates (mL/min, from left to right): 200:0 (pure N_2); 150:50, 100:100, 50:150 and 0:200 (pure CO_2). The total pressure in the electrolyser was 1 atm.

$$CO_3^{2-} + 2e = CO + 2O^{2-} \quad (E^o = -0.947 \text{ V, A2}) \quad (8)$$
$$CO + 2e = C + O^{2-} \quad (E^o = -1.442 \text{ V, A1'}) \quad (9)$$
$$2CO + O^{2-} = CO_3^{2-} + C \quad (10)$$

Note that (10) = (9) – (8), and it is a chemical reaction. However, the observed small craters in Fig. 2b seem to indicate slower kinetics of reactions (9) and (10), likely because CO was in the gas phase. Also, reactions (8) and (10) suggest that the O^{2-} ions could prevent or reduce formation of CO bubbles, which agrees with the absence of craters on the carbon coatings deposited from carbonate dominated baths as discussed below.

The fairly symmetrical shape of peak C1 in Fig. 1a implies Ni may have some catalytic effect on CO_3^{2-} reduction. It was also observed that the current of the symmetrical peak C1 decreased significantly on the 2nd potential cycle, which may be resulting from the Ni surface being covered by the deposited carbon and hence losing the catalytic effect. On the other hand, the absence of a re-oxidation counterpart of peak C1 suggests irreversibility of carbon deposition in the chloride dominated molten salt bath. This could be related to the CV being recorded under Ar, and that there were too few O^{2-} and/or CO_3^{2-} ions in the chloride dominated molten salt bath to assist carbon oxidation via reaction (11) or (12) below.[6]

$$C + 2O^{2-} = CO_2 + 4e \quad (A1, E^o = -1.488 \text{ V}) \quad (11)$$
$$C + 2CO_3^{2-} = 3CO_2 + 4e \quad (A3, E^o = -1.025 \text{ V}) \quad (12)$$

It was then thought that if the CVs were recorded in a carbonate dominated molten salt bath under CO_2, carbon deposition and re-oxidation of the deposited carbon could be both facilitated. To confirm this, the molten eutectic mixture of Li_2CO_3–K_2CO_3 (molar ratio: 62:38) was used to record CVs.[11] Note that the Ni wire was replaced by a Pt wire which can offer a greater stability at more positive potentials to allow studies of all possible anodic reactions. Also, an alumina membrane Ag/AgCl reference electrode was used to offer a more stable reference potential.[16]
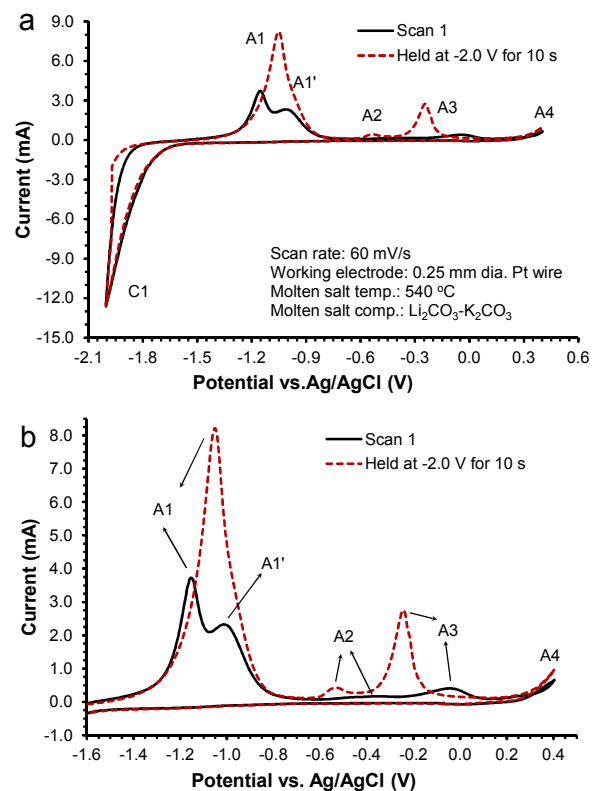

Fig. 3. CVs of a Pt wire (0.25 mm dia.) in molten Li_2CO_3-K_2CO_3 (62:38 mol. ratio) at 540 °C; scan rate :100 mV/s. (a) Full potential range. (b) Enlargement of the anodic branch of the same CVs in (a).

Typical CVs obtained in Li_2CO_3–K_2CO_3 are presented in Fig. 3. The potential window is about 1.90 V between the current onset potentials of peaks C1 (-1.65 V vs. Ag/AgCl) and A4 (0.25 V vs. Ag/AgCl) measured in Fig. 3a. This is slightly wider than that of pure Li_2CO_3 (1.72 V, Table 1), but it is understandable considering the influence of K_2CO_3. The CVs present a significant reduction peak C1, and several re-oxidation peaks as highlighted in Fig. 3b. To confirm these anodic peaks to be indeed due to re-oxidation of the deposited carbon, the potential was held at the cathodic limit (-2.0 V) for 10 s before the scan was reversed. In response, all anodic peaks increased significantly in current, whilst peak A1' was engulfed in A1. This phenomenon can be explained as follow. More

carbon was deposited when the potential was hold at -2.0 V and hence contributed to greater re-oxidation currents. According to their relative potentials, peaks A1 and A3 could be attributed to reactions (11) and (12), respectively. Peaks A1' and A2 were likely the reverses of reactions (9) and (8), respectively, considering their potentials relative to that of A1 for reaction (11). Interestingly, both peaks A2 and A3 have shifted negatively after holding the potential scan at -2.0 V for 10 s. It is very likely that when CO is produced after peak A1' via the reverse of reaction (9), it adsorbs on the carbon surface, impeding reaction (12) and hence a more positive potential for peak A3. Thus, the absence of A1' on the CV after holding the potential at -2.0 V means a lowered influence of CO, and hence the negative shift of A3. If peak A2 corresponds to the reverse of reaction (8), its negative shift may results from a smaller number and size of the CO nuclei on the deposited carbon.

The oxidation current, A4, at the anodic potential limit (0.5 V) may be attributed to the discharge of either the O^{2-} ion to form O_2 (13), or the CO_3^{2-} ion to O_2 and CO_2 (5).

$$2O^{2-} = O_2 + 4e \qquad (E^o = -0.463 \text{ V}) \quad (13)$$

If reaction (13) occurred, its current should have appeared at potentials between A3 and A4 on the CV. However, for reaction (13) to proceed, a significant amount of O^{2-} ions should be present near the electrode. This was unlikely the case, considering that the O^{2-} ions, including those already present in the molten carbonate salts and those produced during carbon deposition via reaction (6), should have been mostly consumed in the course of potential scan from A1 to A3. Thus, A4 should correspond to reaction (5).

Having obtained the basic understanding of the CV, further analysis was carried out to study the feasibility of employing the carbon deposition and dissolution processes for electrochemical energy storage and reuse. This effort started in this work by comparing the charges passed during the cathodic and anodic potential scans when recording the CVs. Some of the results obtained are listed in Table 2.

Table 2. Ratio of anodic (Q^+) and cathodic (Q^-) charges measured from CVs (cf. Fig. 3) as a function of potential scan rate.

Scan rate (mV/s)	Q^- (C)	Q^+ (C)	Q^+/Q^-
100	3.575	1.776	0.50
80	6.220	3.151	0.51
60	6.524	3.362	0.52
40	10.75	5.737	0.53
20	25.56	14.41	0.56
10	73.56	47.70	0.65

Note: All measurements were made using a fresh Pt working electrode in the same molten salt bath.

As it can be seen in Table 2, the Q^+/Q^- ratio increased with decreasing the potential scan rate. In line with this trend, it was found that holding the potential for 10 s at the cathodic end could further increase the Q^+/Q^- ratio close to 1. These observations imply that carbon deposition may not proceed well on the fresh Pt electrode, but becomes more efficient (although not necessarily quicker) after the Pt electrode is covered by the deposited carbon. In other words, carbon deposition on the Pt surface may proceed in competition with other reactions whose products do not remain on the electrode (e.g. CO formation), but these side reactions encounter higher kinetic barriers on the carbon surface. This understanding is practically important because it basically means that for electro-deposition of carbon, the cathode material can be any metal or alloy as long as it is cathodically stable in the molten salt.

To further study electro-oxidation of the deposited carbon, the potentiostatic control was applied to produce a sufficient amount of carbon deposit for further analyses. Particularly, chronopotentiometry was carried out to confirm reactions (11) and (12) as the main anodic reactions on the deposited carbon. In these experiments, the working electrode was a 5 mm dia. mild steel rod, whilst graphite, SnO_2 and stainless steel were all tested as the counter electrode material, and similar results were obtained. However, stainless steel was proven to be the most convenient choice for various carbonate dominated baths, although minor anode dissolution and consequent contamination of the deposited carbon were observed.[11] Thus, the following discussion will focus on data obtained from using the stainless steel counter electrode.

Fig. 4 compares the chronopotentiometric plots recorded during anodic oxidation (dissolution or galvanostatic discharge) of the electro-deposited carbon obtained under potentiostatic control. Both pure Li_2CO_3 and Li_2CO_3-K_2CO_3 were tested for comparison. On all plots in Fig. 4, there are two clearly distinguishable plateaux at potentials corresponding approximately to those of reactions (11) and (12). In Fig. 4b and 4c, a third potential plateau is shown at a more positive potential. The potential difference between the lowest and highest plateaux is about 1.75 V which can be explained by polarisations in addition to the theoretical value of 1.488 V between reactions (5) and (11). Polarisation is evident by a comparison between Fig. 4a and 4b. The potential difference between the first and second plateaux is about 0.40 V in Fig. 4a, but it increases to about 0.78 V in Fig. 4b. The larger current and lower temperature for recording Fig. 4b would have contributed to increasing both the ohmic and charge transfer polarisations. Thus, the third plateau can be attributed to reaction (5), i.e. electro-oxidation of the CO_3^{2-} ion.

Similar to the CVs in Fig. 3 which indicate no clear presence of direct anodic discharge of the O^{2-} ion, i.e. reaction (13), the plots in Fig. 4 show also only a barely visible inflexion on the fast increasing current between the 2nd and 3rd plateaux. This is understandable because of the O^{2-} activity must be significantly lower than that of the CO_3^{2-} ion in the used molten carbonate salts. Also, these experiments were carried out under CO_2 which could also help convert O^{2-} to CO_3^{2-}.

For energy storage, a high Q^+/Q^- ratio approaching 1 is desirable. Cyclic voltammetry has revealed promising results as shown in Table 2. More analyses were carried out on carbon coatings deposited under potentiostatic control and discharged

Table 3. Ratio of Q^+/Q^- as a function of carbon deposition potential (E vs. Ag/AgCl), deposition charge (Q^-), re-oxidation current (I), measured in molten Li_2CO_3-K_2CO_3 (62:38, mol. ratio) at 700 °C under CO_2.

E (V)	Q^- (C)	I (mA)	Q^+/Q^-, 1st plateau	Q^+/Q^-, 2nd plateau
-1.68	1017	150	0.26	0.83
-1.68	973.6	300	0.17	0.48
-1.68	1301	450	0.18	0.34
-1.98	1764	300	0.16	0.32
-2.28	2318	300	0.15	0.28

(re-oxidised) via chronopotentiometry. Some of the preliminary findings are presented in Table 3.

The Q^+/Q^- ratio was found to be a complex function of both deposition and re-oxidation variables. The deposition potential (and voltage if in a two-electrode cell) plays the most significant role. With increasing negatively the deposition potential, the Q^+/Q^- ratio decreases quickly. This trend can be explained by parasitic reactions (e.g. CO formation) in competition with carbon deposition. Temperature change has a relatively small effect on the Q^+/Q^- ratio.

Increasing the deposition charge has a negative effect on the Q^+/Q^- ratio, whilst decreasing the re-oxidation current is beneficial. These can be related to the fact that the electro-deposited carbon is composed of various nanoparticulates, instead of a dense continuum.[11] Thus, carbon loss from the electrode with a thick carbon coating is highly likely during electro-oxidation, particularly considering the disturbance from CO_2 bubbles leaving the electrode at high re-oxidation currents.

It was observed in some cases that the overall Q^+/Q^- ratio would be higher if it is so at the end of the first re-oxidation plateau (cf. Fig. 4 and Table 3). The first plateau corresponds to reaction (11) which produces one CO_2 molecule at the expense of four electrons. At the second plateau, reaction (12) also involves four electrons, but creates three CO_2 molecules. Thus, CO_2 disturbance would be more significant at the second plateau than the first one, likely contributing to more non-electrochemical loss of carbon and hence the lower overall Q^+/Q^- ratio. Unfortunately, reaction (11) consumes O^{2-} ions supplied to the electrode surface via diffusion which limits the maximum reaction rate. On the contrary, the CO_3^{2-} ion in reaction (12) is a component of the molten carbonate salts and hence cannot be depleted at the electrode surface. Thus, to promote reaction (11) and mitigate the impact from CO_2 disturbance during re-oxidation (discharge), a well-balanced engineering design of the bath composition, and electrode and cell structures is crucial.

Prospects

According to Fig. 4, the oxidation of carbon should proceed ideally along the lowest potential plateau for reaction (11) that requires sufficient activity of the O^{2-} ion. This is however difficult, if not impossible, to achieve in molten Li_2CO_3 or
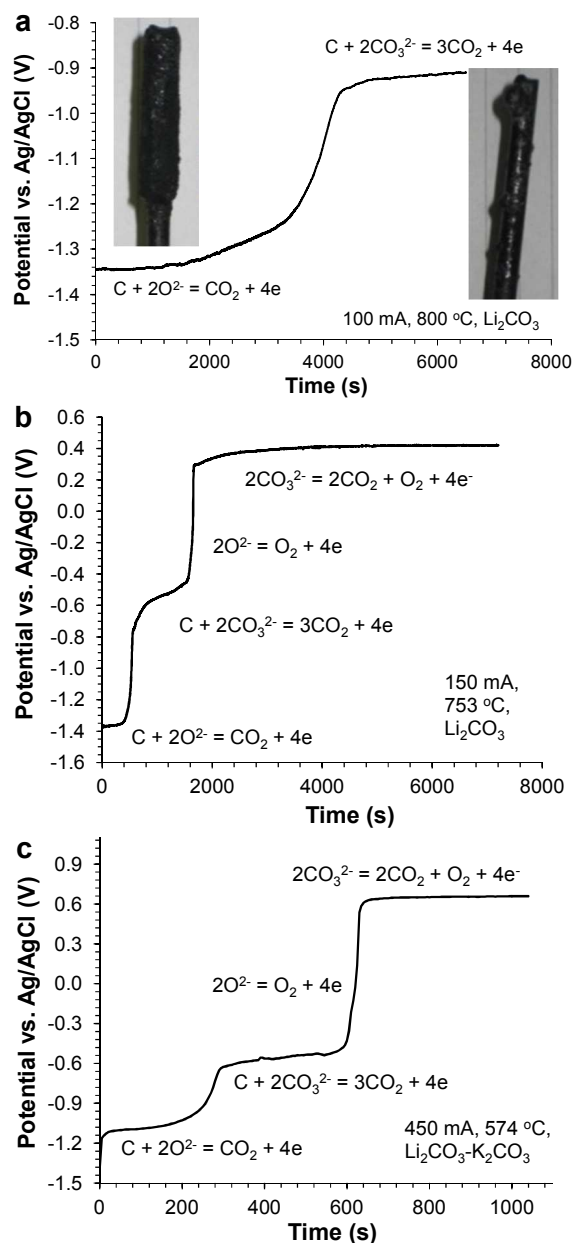

Fig. 4. Chronopotentiometric plots for anodic oxidation of electro-deposited carbon in the same molten salt under CO_2. (a) Li_2CO_3 at 800 °C. Oxidation: 100 mA. Deposition: -1.8 V vs. Ag/AgCl, 3600 s. (b) Li_2CO_3 at 753 °C. Oxidation: 150 mA. Deposition: -2.1 V for 600 s. (c) Li_2CO_3-K_2CO_3 (molar ratio: 62:38) at 574 °C. Oxidation: 450 mA. Deposition: -2.6 V for 600 s. The photographs in (a) show the working electrode (5 mm dia. mild steel rod) with the carbon deposit (left), and after anodic oxidation (right), respectively. Counter electrode: 10 mm diameter graphite rod.

mixed Li_2CO_3-K_2CO_3 under a CO_2 containing atmosphere. Thus, future work should include studies of carbon deposition and dissolution in molten salts with added alkali or alkaline earth metal oxides (Li_2O and CaO). Apparently, at sufficiently high activities of the O^{2-} ion, reaction (11) (E^o = -1.488 V) may

change to the reverse of reaction (6) (E^o = -1.719 V) at a more negative potential. This is desirable from the viewpoint of carbon oxidation in a battery or fuel cell. On the other hand, however, because a high O^{2-} activity in the molten salt does not favour electro-deposition of carbon via reaction (6) (nor the reduction of O_2 gas in a direct carbon fuel cell), a careful balance is needed.

In addition to energy storage through electrochemical deposition and dissolution, the process of, and products from indirect electro-reduction of CO_2 to carbon can have other applications. For example, the deposited carbon can be used directly for making electrodes of supercapacitors,[10] or after a proper treatment for pollutant absorption. The process itself may be used to convert the CO_2 gas back to the O_2 gas, and hence support lives in the space, undersea or mines. It is thus worth an estimation of the cost of the electro-deposition itself. In this work, very high current efficiency (e.g. 95%) has been achieved in carbonate dominated baths. However, a voltage at or higher than 4.0 V was found to be necessary for electrolysis in the two-electrode cell,[11] which is much higher than the thermodynamic predicted voltage as shown in Table 1. A possible reason is the relatively low activity of O^{2-} ions in the carbonate dominated bath under CO_2 that invokes reaction (5) instead of (13) as the anode reaction. Thus, it is reasonable to predict that the electrolysis voltage can be reduced to below 3.0 V if either Li_2O or CaO is added to the molten salts. Thus, assuming a cell voltage of 3.0 ~ 4.0 V and 95% in current efficiency, the energy consumption in electrolysis can be derived to be 28.2 ~ 37.6 Wh/kg-C, which can be translated to a cost less than \$5/kg-C considering a 20% margin for heating and pre- and post-processing. For comparison, the current market price for supercapacitor grade activated carbon falls in the range of \$20 ~ 40/kg-C.

Summary

Electrochemical deposition and dissolution of carbon can be achieved in carbonate containing molten salts. The deposition becomes faster when CO_2 is present in the atmosphere above the molten salts. The cathodic process is dominated by carbon deposition at high current efficiency (up to 95%), whilst CO formation and other reactions may also occur. It was observed that carbon deposition occurs on the deposited carbon more efficiently than on a freshly prepared metal electrode. Electro-re-oxidation of the deposited carbon can be achieved with the aid of either the preferred O^{2-} ion, or the CO_3^{2-} ion at a more positive potential. Both chronopotentiometry and cyclic voltammetry and revealed a fairly high ratio of deposition and dissolution charges, but also a large difference between the carbon deposition and dissolution potentials. A brief analysis of the process suggests addition of the O^{2-} ion in the form of either Li_2O or CaO in the molten salts may not only benefit to decreasing the electrolysis voltage by avoiding direct anodic oxidation of the CO_3^{2-} ion, but also enable anodic oxidation of the deposited carbon at more negative potentials.

Acknowledgements

Notes and references

Department of Chemical and environmental Engineering, and Energy and Sustainability Research Division, Faculty of Engineering, University of Nottingham, University Park, Nottingham NG7 2RD UK.
Email: george.chen@nottingham.ac.uk

1 Yu. K. Delimarskii, O. V. Gorodiskii and V. F. Grishchenko, *Dokl. Akad. Nauk SSSR*, 1964, **156**, 650–651.

2 M. D. Ingram, B. Baron and G. J. Janz, *Electrochim, Acta*, 1966, **11**, 1629–1639.

3 H. Kawamura and Y. Ito, *J. App. Electrochem.*, 2000, **30**, 571–574.

4 L. Massot, P. Chamelot, F. Bouyer and P. Taxil, *Electrochim. Acta*, 2003, **48**, 465–471.

5 H. Groult, B. Kaplan, F. Lantelme, S. Komaba, N. Kumagai, H. Yashiro, T. Nakajima, B. Simon and A. Barhoun, *Solid State Ionics*, 2006, **177**, 869-875.

6 K. Le Van, H. Groult, F. Lantelme, M. Dubois, D. Avignant, A. Tressaud, S. Komaba, N. Kumagai and S. Sigrist, *Electrochim. Acta*, 2009, **54**, 4566–4573.

7 S. Licht, B. Wang, S. Ghosh, H. Ayub, D. Jiang and J. Ganley, *J. Phys. Chem. Lett.*, 2010, **1**, 2363-2368.

8 N. J. Siambun, H. Mohamed, D. Hu, D. Jewell, Y. K. Beng and G. Z. Chen, *J. Electrochem. Soc.*, 2011, **158**, H1117–H1124.

9 Q. S. Song, Q. Xu, Y Wang, X. J. Shang and Z. Y. Li, *Thin Solid Films*, 2012, **520**, 6856–6863.

10 H. Yin, X. Mao, D. Tang, W. Xiao, L. Xing, H. Zhu, D, Wang and D. R. Sadoway, *Energy Environ. Sci.*, 2012, **6**, 1538–1545.

11 H. V. Ijije, C. Sun and G. Z. Chen, *Carbon*, 2014, DOI: 10.1016/j.carbon.2014.02.052

12 M. Tahir, N. S. Amin, *Energy Conversion and Management*, 2013, **76**, 194-214.

13 *HSC Chemistry 6*, v. 6.12, Outotec Research Oy, 2007.

14 G. Z. Chen, *A feasibility study of solar-electrochemical cells for capturing atmospheric carbon*, Application for The Royal Society 2007 Brian Mercer Feasibility Award, October 2006.

15 I. A. Novoselova, N. F. Oliinyk, S. V. Volkov, A. A. Konchits, I. B. Yanchuk, V. S. Yefanov, S. P. Kolesnik, M. V. Karpets, *Physica E*, 2008, **40**, 2231-2237.

16 R. Barnett, K. T. Kilby, D. J. Fray, *Metall. Mater. Trans. B*, 2009, **40**, 150-157.

17 H. Wang, N. J. Siambun, L. P. Yu and G. Z. Chen, *J. Electrochem. Soc.*, 2012, **159**, H740–H746.

ToC Graphic and text

Energy from sunlight in summer can be stored in carbon via facile electrochemical reduction of carbon dioxide in molten salts, and then discharged in winter aided by oxygen as heat or electricity via a fuel cell or battery with the same molten salts as the electrolyte.